Nucleation and Growth Mechanisms of Fe Oxyhydroxide in the Presence of PO 4 Ions. 1. Fe KEdge EXAFS Study

ARTICLE *in* LANGMUIR · DECEMBER 1996

Impact Factor: 4.46 · DOI: 10.1021/la9606299

Nucleation and Growth Mechanisms of Fe Oxyhydroxide in the Presence of PO_4 Ions. 2. P K-Edge EXAFS Study

Jérôme Rose,[†] Anne-Marie Flank,[‡] Armand Masion,[†] Jean-Yves Bottero,*[,†] and Pierre Elmerich[§]

Laboratoire des Géosciences de l'Environnement URA 132 CNRS et Univ. Aix-Marseille III, CEREGE FU 017, BP 80, Europole Méditerranéen de l'Arbois, 13545 Aix-en-Provence Cedex 4, France, Laboratoire pour l'Utilisation du Rayonnement Electromagnétique, Centre Universitaire Paris-Sud, 91405 Orsay Cedex, France, and Elf-Atochem. Centre d'application de Levallois, 95 rue Danton, 92300 Levallois-Perret, France

Received October 24, 1996[⊗]

P K-edge EXAFS spectroscopy has been used to determine the local environment of phosphorus during the hydrolysis of $FeCl_3$ in the presence of phosphate. Measurements were performed on liquid samples and in the fluorescence mode. With the detection geometry adopted during experiments, the self absorption of fluorescence has been quantified and does not appear to be an important phenomenon. Thus no correction was made. In order to clearly identify the neighboring atoms around P, a multiple scattering approach has been used. Multiple scattering seems to be an important phenomenon in $PO_4/FeCl_3$ clusters. P K-edge EXAFS data show that even for very acidic solutions, pH < 1, all the phosphate ions are complexed to Fe. For a P/Fe molar ratio of 0.2 one phosphate progressively bonds one, two, and three irons when n (=[OH]/[Fe]) increases from 0 to 2.0. At $n = 2$, one phosphate bridges three iron dimers and two kinds of PO_4−Fe linkages are detected. For P/Fe = 0.5, the number of irons linked to PO_4 increases when n increases but does not exceed 2. Thus P K-edge EXAFS spectroscopy combined with a multiple scattering approach allowed us to confirm previous results obtained by EXAFS at the Fe K-edge as well as to describe more precisely the type of linkage between the PO_4 tetrahedron and the Fe octahedra.

Introduction

The hydrolysis of iron is an important process in the geochemical cycle of iron in the supergene environment. This spontaneous phenomenon leads to the formation of amorphous precipitates.[1−3] The hydrolysis and growth of iron species in natural fresh water are poorly understood. The presence of an inorganic ligand such as PO_4, SiO_4, or SO_4 competing with O or OH strongly modifies the normal pathway of iron hydrolysis. PO_4 ions hinder the hydrolysis of Fe^{3+} cations by affecting the size and crystallinity of the particles even at low [PO_4]/[Fe] molar ratios.[4] Similar results were obtained with titanium.[5] In a previous work, the very first steps of the hydrolysis of Fe(III) in the presence of PO_4 ions were studied by Fe K-edge EXAFS spectroscopy.[6] It appeared that the hydrolysis of Fe(III) is blocked at the edge-sharing iron dimer stage. The growth of the colloids is achieved by PO_4 bridging Fe dimers.

At P/Fe = 0.2, the average number of PO_4, N_p, in the second coordination sphere of Fe atoms is 0.4 and 0.6 for hydrolysis ratios n = [OH]/[Fe] of 1.5 and 2.0, respectively. This means that one PO_4 bonds two Fe dimers at $n = 1.5$ and three Fe dimers at $n = 2$. At P/Fe = 0.5, the number N_p is always equal to 1. This implies that one PO_4 bridges two iron dimers. For P/Fe = 0.2 and $n = 1.0$, the presence of PO_4 in the coordination sphere of iron was not detected.

The difficulty in determining the presence of P in the local environment of Fe using Fe K-edge EXAFS spectroscopy arises from the great difference in atomic numbers of these elements: the amplitude function for Fe−Fe is higher than that for the Fe−P atomic pair. Thus, it is sometimes very difficult to detect a Fe−P contribution to the EXAFS signal.

In the present paper we aim at overcoming this difficulty by using P K-edge EXAFS spectroscopy on the solutions and suspensions in order to determine the local structure of P atoms 'in situ' and thus specify the influence of the PO_4 ligand on the $FeCl_3$ hydrolysis. The results are compared with those obtained by Fe K-edge EXAFS on the same samples, which are reported in a companion paper.[6]

Materials and Methods

Materials. The samples investigated in the present work were the same as those previously used for a Fe K-edge EXAFS study.[6] Briefly, Fe/PO_4 mixtures ([P]/[Fe] = 0.2 and 0.5 and [Fe] = 1.5 M) were slowly hydrolyzed using 10 M sodium hydroxide until hydrolysis ratios n = [OH]/[Fe] of 1.0, 1.5, and 2.0 were reached.

Methods. *X-ray Absorption Spectroscopy.* P K-edge EXAFS measurements were performed at room temperature in the fluorescence mode at the Super-ACO synchrotron (Orsay, France) on the EXAFS SA 32 beamline equipped with a double-crystal (Ge(111)) monochromator (P K-edge = 2149 eV). The positron storage ring was running at 0.8 GeV with a typical current of 200 mA. The incident beam was monitored by measuring the total electron drain current on an aluminum foil located downstream of the monochromator. In the soft X-ray region the measurement of X-ray absorption coefficient using the transmission mode is not applicable, since it would require very thin cells (≈1 μm) and homogeneous samples.[7] Moreover this method is not applicable to dilute absorbing elements (samples where the absorption due to the central atom is much smaller compared to the absorption

[†] Laboratoire des Géosciences de l'Environnement URA 132 CNRS et Univ. Aix-Marseille III.

[‡] Centre Universitaire Paris-Sud.

[§] Elf-Atochem. Centre d'application de Levallois.

[⊗] Abstract published in *Advance ACS Abstracts,* February 15, 1997.

(1) Tchoubar, D.; Bottero, J. Y.; Quienne, P.; Arnaud, M. *Langmuir* **1991**, *7*, 398−402.

(2) Bottero, J. Y.; Tchoubar, D.; Arnaud, M.; Quienne, P. *Langmuir* **1991**, *7*, 1365−1369.

(3) Combes, J. M.; Manceau, A.; Calas, G.; Bottero, J. Y. *Geochem. Cosmochim. Acta* **1989**, *53*, 583−594.

(4) Kandori, K.; Uchida, S.; Kataoka, S.; Ishikawa, T. *J. Mater. Sci.* **1992**, *27*, 719−728.

(5) Schmutz, C.; Barboux, P.; Ribot, F.; Tautelle, F.; Verdaguer, M.; Fernandez-Lorenzo, C. *J. Non-Cryst. Solids* **1994**, *170*, 250−262.

(6) Rose, J.; Manceau, A.; Bottero, J. Y.; Masion, A.; Garcia, F. *Langmuir* **1996**, *12*, 6701−6707.

(7) Tröger, L.; Arvanitis, D.; Baberschke, K.; Michaelis, K.; Grimm, U.; Zschech, E. *Phys. Rev.* **1992**, *46* (6), 3283−3289.

S0743-7463(96)01039-6 CCC: $14.00

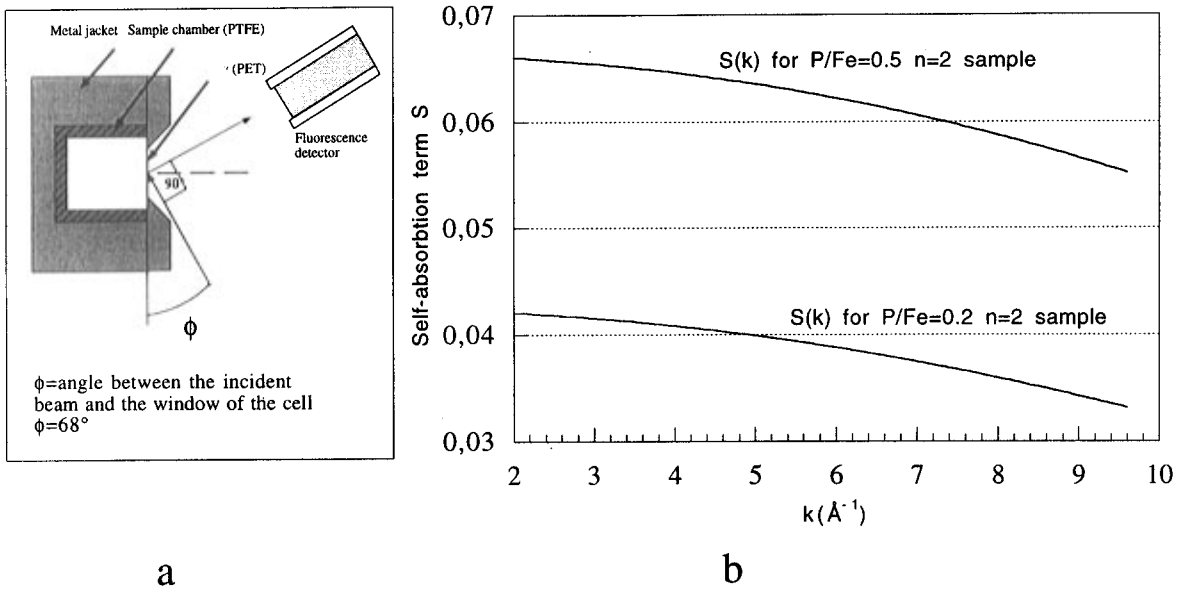

Figure 1. (a) Experimental setup. The detection geometry is characterized by Φ (angle of the incident beam with the sample surface). (b) Self-absorption term S vs k for $Fe_3O_{16}PCl_3$ (P/Fe = 0.2, n = 2) and $Fe_2O_{12}PCl_2$ (P/Fe = 0.5, n = 2) for one detection geometry (Φ = 68°).

of the other atoms within the sample). Thus for dilute samples and for 'in situ' analysis of solution, the absorption is often measured indirectly by monitoring the decay of the core electron hole by X-ray fluorescence. In those cases the fluorescence yield is directly proportional to the absorption coefficient of the central atom and therefore the extraction of the EXAFS data is straightforward. The fluorescence yield was measured using an intrinsic low energy germanium monoelement located at 90° to the incident beam.

In order to carry out "in situ" analysis of our corrosive solutions, we designed a special sample holder enabling EXAFS measurements in the fluorescence mode. It was imperative that the cell could withstand the high vacuum required for EXAFS studies in the soft X-ray region. The sample chamber was made of polytetrafluoroethylene (PTFE), having a window wherein a 5 μm thick polyethylene terephthalate (PET) film is adjusted. A metal jacket encloses both the window and sample chamber (Figure 1b). An O ring is placed between the window and the chamber cell. The design of the cell allows the angle between the X-ray beam and the sample surface to vary from 20 to 70°, which corresponds to the optimum setup for fluorescence measurements.[6] The corrosive solution is in contact only with PTFE and PET.

Data Reduction. Absorption spectra were obtained by averaging 6−10 experimental spectra. In fluorescence experiments, the background $\mu_0(E)$ generally increases with increasing energy E; the positive slope of $\mu(E)$ vs E is due to the fact that as the photon energy increases, the X-ray beam penetrates deeper into the sample, thereby producing more fluorescence signals.[8] Concerning the EXAFS part of the spectra, the data analysis was performed in a classical way: the oscillatory part was extracted using a 'spline' function fit and normalized using an Heitler approximation.[9]

A Kaiser window (τ = 2.5) was then applied to the $k^z\chi(k)$ weighted data before Fourier transforming from k = 1.7 up to 10.5−11 Å^{-1} (E = 12−550 eV), where k stands for the modulus of the wave vector (expressed in Å^{-1}) associated with the electronic wave. A z value of 1 was used in order to minimize the weight of background noise of the high-energy region of each spectrum. All the Fourier transforms (radial distribution functions: RDFs) are uncorrected for phase shift; i.e., RDF peaks are translated from crystallographic distances by ≈0.3−0.4 Å.

The structural and chemical parameters for each atomic pair (N_j (number of atoms in the jth shell), R_j (distance between the central atom and the atom in the jth shell), and σ_j (Debye−Waller factor, which accounts for thermal vibrations and static disorder)) were determined according to a procedure previously described.[6]

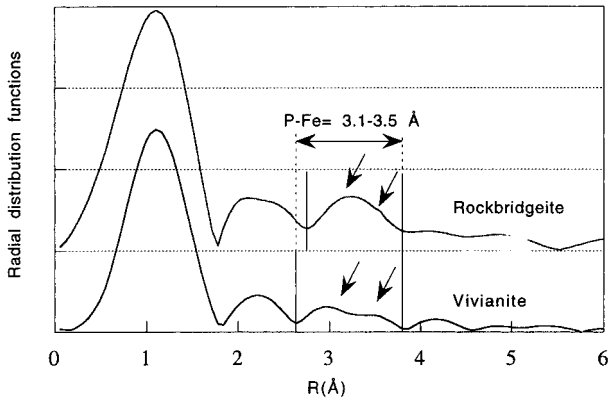

Figure 2. RDF of reference minerals. Arrows indicate the peaks corresponding to P−Fe and P−O[second neighbors] contributions in well crystallized iron/phosphate.

Determination of the Empirical Amplitude and Phase Functions. For the different atomic pairs, the amplitude functions F_{P-O} and F_{P-Fe}, which depend on the atoms in the jth shell (O or Fe) and the phase shift functions of the P−O or P−Fe pairs (ϕ_{P-O}, ϕ_{P-Fe}) were determined using theoretical functions.[10] They were validated with pure and well-crystallized iron phosphate references: vivianite,[11] and rockbridgeite.[12] Figure 2 shows the RDFs of the two references used. The first peak corresponds to the first coordination shell of phosphorus, which is constituted by four oxygen atoms at an average distance of 1.54 Å for vivianite[11] and 1.53 Å for rockbridgeite.[12] The region in which F_{P-O}, F_{P-Fe}, ϕ_{P-O}, and ϕ_{P-Fe} were validated is indicated by arrows. For both references, the 2.6/2.7−3.8 Å range corresponds to the presence of two peaks (vivianite) or one peak and one shoulder (rockbridgeite). The first peak (2.6−3.4 Å in vivianite and 2.7−3.5 Å in rockbridgeite) corresponds to the presence of P−Fe and P−O shells, and the second contribution corresponds to P−O shells. Because these two peaks are not well separated, it was not possible to fit each peak separately. For unknown samples, P−Fe distances are expected in the range 3.1−3.5 Å,[6] as in vivianite and rockbridgeite. The 2.6/2.7−3.4/3.5 Å region (distances uncorrected for phase shift) of experimental spectra was thus carefully analyzed.

EXAFS parameters determined from iron phosphate references are listed in Table 1. The uncertainties on R and N are ±0.06

(8) Teo, B. K. *Inorganic Chemistry Concepts*; Springer-Verlag: Berlin, 1986.
(9) Lengeler, B.; Eisenberger, P. *Phys. Rev.* **1980**, *B21*, 4507.
(10) McKale, A. G.; Veal, B. W.; Paulikas, A. P.; Chan, S. K.; Knapp, G. S. *J. Am. Chem. Soc.* **1988**, *110*, 3736.
(11) Fedji, P.; Poullen, J. F. *Bull. Mineral.* **1980**, *103*, 135−138.
(12) Moore, P. B. *Am. Mineral.* **1970**, *55*, Jan−Feb.

Table 1. Crystallographic and EXAFS Parameters of Reference Minerals

			P−Fe$_1$ shell[a]			P−Fe$_2$ shell[a]				P−O$_2$ shell[b]			P−O$_3$ shell[b]				
R window[e] (Å)	sample		R_{Fe1} (Å)	N_{Fe1}[f]	σ_{P-Fe1} (Å)	R_{Fe2} (Å)	N_{Fe2}	σ_{P-Fe2} (Å)	L[c] (Å^{-2}) (P−Fe)[d]	R_{O2} (Å)	N_{O2}	σ_{P-O2} (Å)	R_{O3} (Å)	N_{O3}	σ_{P-O3} (Å)	L (Å^{-2}) (P−O)[d]	Q[g]
2.6−3.8	Vivianite	EXAFS	3.24	3	0.080	3.44	2	0.085	1.8	3.42	5	0.105	3.63	5	0.100	2.3	0.003
		XRD	3.23	3		3.41	2			3.42	5		3.67	5			
2.7−3.8	Rockbridgeite	EXAFS	3.1	2	0.110	3.34	6	0.115	1.8	3.62	6	0.100				2.3	0.007
		XRD	3.13	2		3.30	6			3.56	6						

[a] P−Fe$_1$ and P−Fe$_2$ correspond to the first and second P−Fe shells, respectively. [b] P−O$_2$ and P−O$_3$ correspond to the second and third P−O shells, respectively. The first P−O shell is not taken into account due to the R window. [c] L corresponds to the first term in the $\lambda(k)$ expression ($\lambda(k) = 2k/L$). [d] ΔE is equal to −1 (eV) and to −15 (eV) for the P−Fe the P−O pairs, respectively. [e] R is the distance between the two atoms of each atomic pair. [f] N is the number of atoms in the 2nd and 3rd spheres of phosphorus. [g] $Q = \sum[(k^3\chi_{theo}) - (k^3\chi_{exp})]^2/(k^3\chi_{exp})^2$.

Å and 10%, respectively. One can observe that σ_{P-Fe} is higher for rockbridgeite (0.11 Å) than for vivianite (0.08 Å). In the reference samples used, the value of σ depends on the number of Fe atoms in the coordination sphere of P, the distance distribution P−Fe, and the choice made to fit the partial EXAFS spectra. For example in the case of rockbridgeite, phosphorus is surrounded by eight iron atoms at six different distances (3.13, 3.22, 3.26, 3.30, 3.33, and 3.37 Å).[12] It is not possible to fit the experimental spectrum using six iron shells. These six P−Fe contributions were separated in two subgroups, and the fitting simulation was carried out using two P−Fe shells (Table 1). This leads to a large distance distribution for both P−Fe shells.

In the case of vivianite, phosphorus is surrounded by five iron atoms at only three different distances (3.20, 3.25, and 3.42 Å).[11] The fit of the partial EXAFS spectrum was assumed using two P−Fe shells. The P−Fe distance distribution for each P−Fe shell (used to fit EXAFS spectra) is thus lower in the case of vivianite than that for rockbridgeite. Accordingly the static disorder part of the Debye−Waller factor σ is lower in vivianite than in rockbridgeite. For the fit of spectra of unknown samples, the σ value of vivianite will be used because, from our previous Fe K-edge results,[6] it appeared that P−Fe distances are not much distributed for clusters present in solution.

In Table 1, σ values relative to P−O shells are equal to 0.1 ± 0.05 Å. Whatever the reference sample, this value is large, because it also results from a large distribution of angles between the Fe−O$_{2\ or\ 3}$ and P−Fe axes.

Concerning the energy edge shift ($\Delta E = E_0$[theory(MacKale] $- E_0$[crystallographic sample]), it was equal to −1 for both P−Fe shells and to −15 for both P−O shells. These values were kept constant for the fitting simulation of partial EXAFS spectra of unknown samples.

Results

Effect of Self Absorption of Fluorescence. The amplitude of EXAFS spectra of samples measured in the fluorescence mode drastically changes with the detection geometry, i.e. the angle between the sample surface and the incident beam. This variation of amplitude is due to the self-absorption of fluorescence by the sample. Recent work[7,13] shows that this difference of amplitude can reach 45% for a NiO EXAFS spectrum obtained with different detection geometries. A classical EXAFS analysis could therefore lead to systematic errors in the determination of structural parameters. In order to avoid this uncertainty about amplitude, the self-absorption of fluorescence can be quantified by comparing the underestimated experimental EXAFS spectrum of phosphorus with a theoretical prediction. The ratio between the experimental phosphorus EXAFS (χ_{exp}) and the theoretical phosphorus spectrum (χ_P) can be written as[7]

$$\chi_{exp}/\chi_P \approx 1 - S(E) - B(E) \qquad (1)$$

with

$$S(E) = \frac{\bar{\mu}_P(E)}{\bar{\mu}_{tot}(E) + \bar{\mu}_{tot}(E_f)g} \qquad (2)$$

where $\bar{\mu}_P(E)$ corresponds to the absorption coefficient of the phosphorus K shell, $\bar{\mu}_{tot}(E)$ is the absorption coefficient for all the elements of the sample, $\bar{\mu}_{tot}(E_f)$ is the absorption coefficient for all the elements of the sample at the phosphorus K_α fluorescence line (2013 eV), and $g = \tan\phi$ is the factor characterizing the experimental detection geometry, with ϕ being the angle between the incident beam and the sample surface or the window of the cell. The term $S(E)$ quantifies the effect of self-absorption on the reduction of amplitude of the experimental EXAFS spectrum and was first given by Goulon et al. in 1982. $B(E)$, which is generally neglected,[7,15] describes the effect of an uncertain background subtraction on the experimental EXAFS.[7] Each absorption coefficient was calculated as follows:[15]

$$\mu_i\ (\mathrm{cm}^{-1}) = \sigma_i\ (\mathrm{barns/atom}) \times \rho_i\ (\mathrm{g/cm}^3) \times N_A(1/A_i) \qquad (3)$$

with A_i the atomic weight of element i, ρ_i the partial density of element i in the material, N_A Avogadro's number, and σ (barns/atom) the photoionization cross sections.[16]

In our case this self-absorption effect was calculated for two samples (P/Fe = 0.2, $n = 2$ and P/Fe = 0.5, $n = 2$). In a first approximation the structures of the colloids determined by Fe K-edge EXAFS[6] were used to determine the parameters A_i and ρ_i.

For P/Fe = 0.2 and $n = 2$, the stoichiometry chosen was $Fe_3PO_{16}Cl_3$. It corresponds to the linkage between one phosphate and three iron octahedra.[6] This small oligomer can be compared with an ellipsoid with three radii of $r_1 = 2.7$ Å, $r_2 = 4.5$ Å, and $r_3 = 5$ Å, having a volume of 250 Å^3. For the calculation of $S(E)$, we used $\phi = 68°$ and $\rho_P(Fe_3PO_{16}Cl_3) = 0.206$ g/cm^3, $\rho_O(Fe_3PO_{16}Cl_3) = 1.700$ g/cm^3, $\rho_{Fe}(Fe_3PO_{16}Cl_3) = 1.316$ g/cm^3, and $\rho_{Cl}(Fe_3PO_{16}Cl_3) = 0.707$ g/cm^3, calculated from the theoretical density $\rho(Fe_3PO_{16}Cl_3) = 3.729$ g/cm^3. The different σ_i(E) curves were determined according to tables given by Yeh et al. For P/Fe = 0.5 and $n = 2$, the stoichiometry of $Fe_2PO_{12}Cl_2$ corresponds to the association of one PO_4 tetrahedron with two Fe octahedra. The volume of the associated ellipsoid is 180 Å^3 ($r = 3$, 3, and 4.9 Å). For the calculation of $S(E)$ we used $\rho_p(Fe_2PO_{12}Cl_2) = 0.286$ g/cm^3, $\rho_O(Fe_2PO_{12}Cl_2) = 1.771$ g/cm^3, $\rho_{Fe}(Fe_2PO_{12}Cl_2) = 1.033$ g/cm^3, and $\rho_{Cl}(Fe_2PO_{12}Cl_2) = 0.655$ g/cm^3, given from the theoretical density $\rho(Fe_2PO_{12}Cl_2) = 3.745$ g/cm^3 and $\phi = 68°$. S was plotted as a function of k. Figure 1 displays $S(k)$ for both samples. $S(k)$ values never exceed 4.2% for P/Fe = 0.2 and $n = 2$ or 6.6% for P/Fe = 0.5 and $n = 2$. It appears from this that

(13) Zschech, E.; Tröger, L.; Arvanitis, D.; Michaelis, H.; Grimm, U.; Baberschke, K. *Solid State Commun.* **1992**, *82*, 1.
(14) Goulon, J.; Goulon-Ginet, C.; Cortes, R.; Dubois, J. M. *J. Phys.* **1982**, *43*, 539.
(15) Pompa, M. Thesis, Universitaire Paris-sud, 1994, Chapters V and VI.
(16) Yeh, J. J.; Lindau, I. *At. Data Nucl. Data Tables* **1985**, *32*, 1.

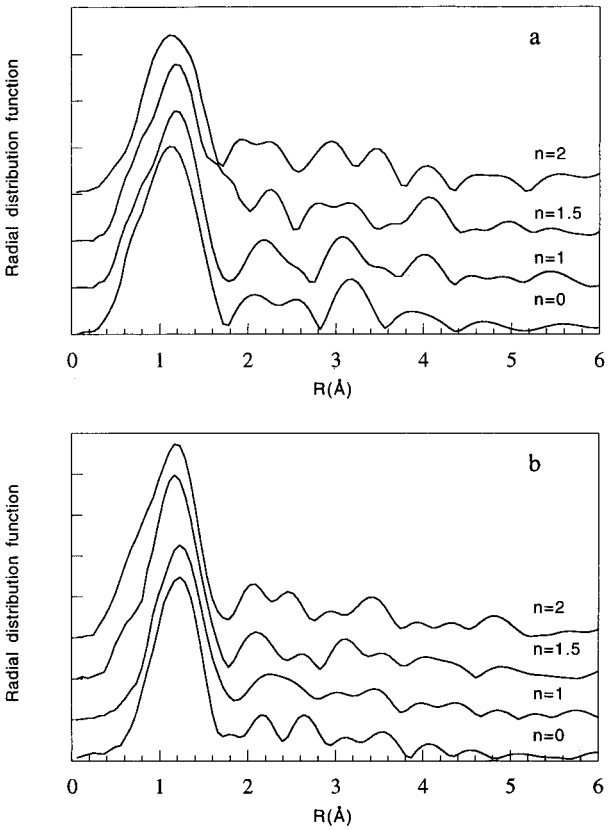

Figure 3. P radial distribution functions (uncorrected for phase shift functions) for (a) P/Fe = 0.2 and (b) P/Fe = 0.5.

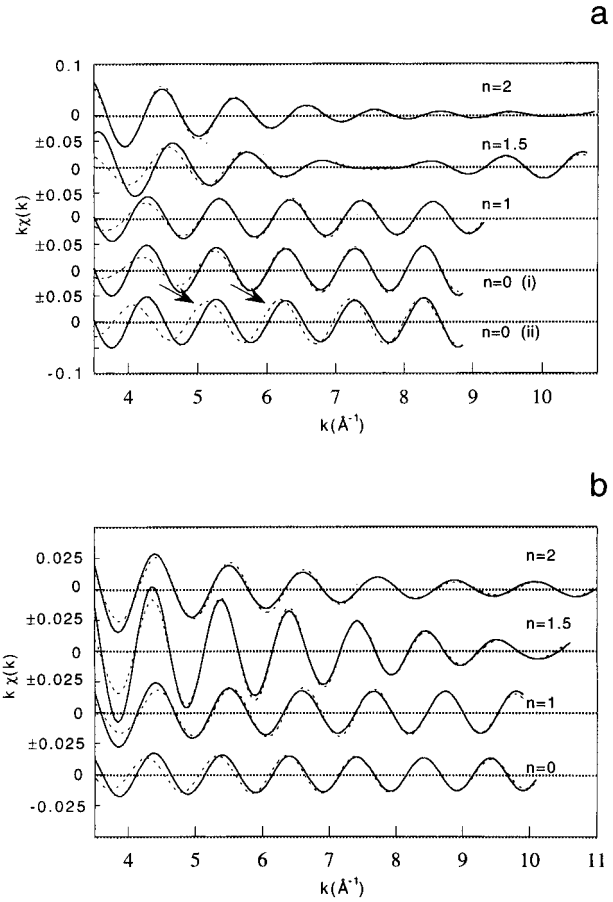

Figure 4. Comparison of partial EXAFS spectra corresponding to the 2nd and 3rd coordination spheres around P: (a) P/Fe = 0.2, $n = 0$ (i), calculation using two shells; $n = 0$ (ii) calculation using one shell; (b) P/Fe = 0.5. Solid line: experimental spectrum. Doted line: calculated spectrum. Arrows indicate differences between experimental and calculated EXAFS curves when only one shell is used.

the self-absorption is not a predominant phenomenon in our case for the samples with the detection geometry we used.

Determination of the Atomic Environment of P through the Analysis of the 2nd and the 3rd Coordination Shell. The radial distribution functions (RDFs) are reported in Figure 3. The first major peak corresponds to the four O atoms constituting the PO_4 tetrahedron. For this first coordination sphere no precise determination of the P−O distances can be extracted from an analysis of the data because the spectra were recorded over a too short energy range. One can note (Figure 3) the presence of one or two peaks in the 1.8−2.7 Å range (distances uncorrected for phase shift). It is difficult to attribute these peaks to structural information, and they could correspond to background noise or multiple scattering effects. This region of the RDFs will be analyzed further. Peaks in the 2.7−3.5 Å range (distances not corrected for phase shift) certainly correspond to P−Fe contributions.

Least-square fitted χ[P(2nd and 3rd backscatterers)]-(k) spectra are compared to experimental ones in Figure 4, and the corresponding structural parameters are reported in Table 2. The fitting of P/Fe = 0.2, $n = 0$ and $n = 1$ was performed by using two atomic shells. The use in addition of a $P-O_2$ shell at 3.4−3.52 Å reproduces the phase shape of the experimental spectra (Figure 4A, $n =$ 0 (i)).

One can observe that σ_{P-Fe} is lower (0.06−0.07 Å) than that in vivianite (0.08 Å) (Table 1).

This small difference could be due to a lower distance distribution P−Fe in the small clusters formed in the present samples.[6]

For P/Fe = 0.2, at n =1.5 and 2, the 2.6−3.3 Å range of the RDF curves, on which back Fourier transforms are applied, corresponds either to two peaks (n = 1.5) or to one peak and a shoulder ($n = 2$) (Figure 2a). This accounts at least for two contributions for each partial EXAFS curve. The recalculation procedure which uses two shells for each partial EXAFS curve therefore seems reasonable. The use of a $P-O_2$ shell increases the accuracy of the phase and amplitude at low k values (Figure 4a, $n = 2$).

For P/Fe = 0.5, the fitting of the partial EXAFS curves (Figure 4b) required only one second atomic shell $P-Fe_1$ for $n = 0$ and $n = 1$ and a second atomic shell $P-O_2$ for $n = 1.5$ and $P-Fe_2$ for $n = 2.0$ (Table 2).

For P/Fe = 0.2, the parameters R_{Fe1}, N_{Fe1}, R_{Fe2}, and N_{Fe2} are generally in good agreement with those obtained from Fe K-edge EXAFS data.[6] However, at $n = 1.5$ and $n = 2.0$, an unusually short $P-Fe_1$ distance of 3.05 Å was detected (Table 2). With increasing hydrolysis ratio, the P−Fe distance decreases from 3.4 to 3.17 Å (on average) and $N_{Fe1} + N_{Fe2}$ increases from 1.6 to 3.2.

Similarly, for the P/Fe = 0.5 series, the structural parameters evolve in the same manner as for P/Fe = 0.2 when n increases and $N_{Fe1} + N_{Fe2}$ is on average close to 2 for $n = 1.5$ and $n = 2$. This is in agreement with the results obtained at the Fe K-edge.

Data obtained at the P K-edge show that two P−Fe distances are detected. A previous study carried out at the Fe K-edge only showed the presence of one Fe−P distance,[6] corresponding to the average value of $P-Fe_1$ and $P-Fe_2$ detected in the present work. The differences between Fe and P K-edge EXAFS data are mainly observed for low hydrolysis ratios. For example, for both series at $n = 0$, Fe K-edge EXAFS data did not allow us to conclude on the presence of atoms in the second coordination sphere of Fe, whereas some associations between Fe and PO_4 can be detected in the present work.

Table 2. Structural Parameters for P (Backscatterers in the 2nd and 3rd Coordination Spheres) Contributions Derived from EXAFS Analysis for P/Fe = 0.2 and P/Fe = 0.5

		P−Fe_1 shell			P−Fe_2 shell				P−O_2 shell				
sample	*R* window[a] (Å)	R_{Fe1} (Å)	N_{Fe1}	σ_{P-Fe1} (Å)	R_{Fe2} (Å)	N_{Fe2}	σ_{P-Fe2} (Å)	ΔE (eV) P−Fe	R_{O2} (Å)	N_{O2}	σ_{P-O2} (Å)	ΔE (eV) P−O	*Q*
P/Fe = 0.2													
n = 0	2.8−3.4	3.39	1.6	0.065				−1,5	3.42	2.1	0.095	−16	0.009
n = 1	2.7−3.4	3.35	1.7	0.060				0	3.40	1.6	0.095	−15	0.006
n = 1.5	2.6−3.3	3.05	1.0	0.070	3.30	1.4	0.060	−1	3.30	2.3	0.095	−16	0.017
n = 2	2.6−3.3	3.06	1.3	0.060	3.24	1.9	0.060	0	3.42	2.5	0.095	−15	0.015
P/Fe = 0.5													
n = 0	2.9−3.3	3.35	0.7	0.065				−1				−16	0.015
n = 1	2.9−3.3	3.24	0.8	0.065				−1,5				−16	0.008
n = 1.5	2.7−3.4	3.30	2.0	0.070				−1	3.52	2.0	0.105	−16	0.010
n = 2	2.7−3.2	3.15	0.6	0.065	3.31	1.2	0.070	−1				−15	0.020

[a] *R* is the distance between the two atoms of each atomic pair. [b] *N* is the number of atoms in the 2nd and 3rd coordination spheres of phosphorus.

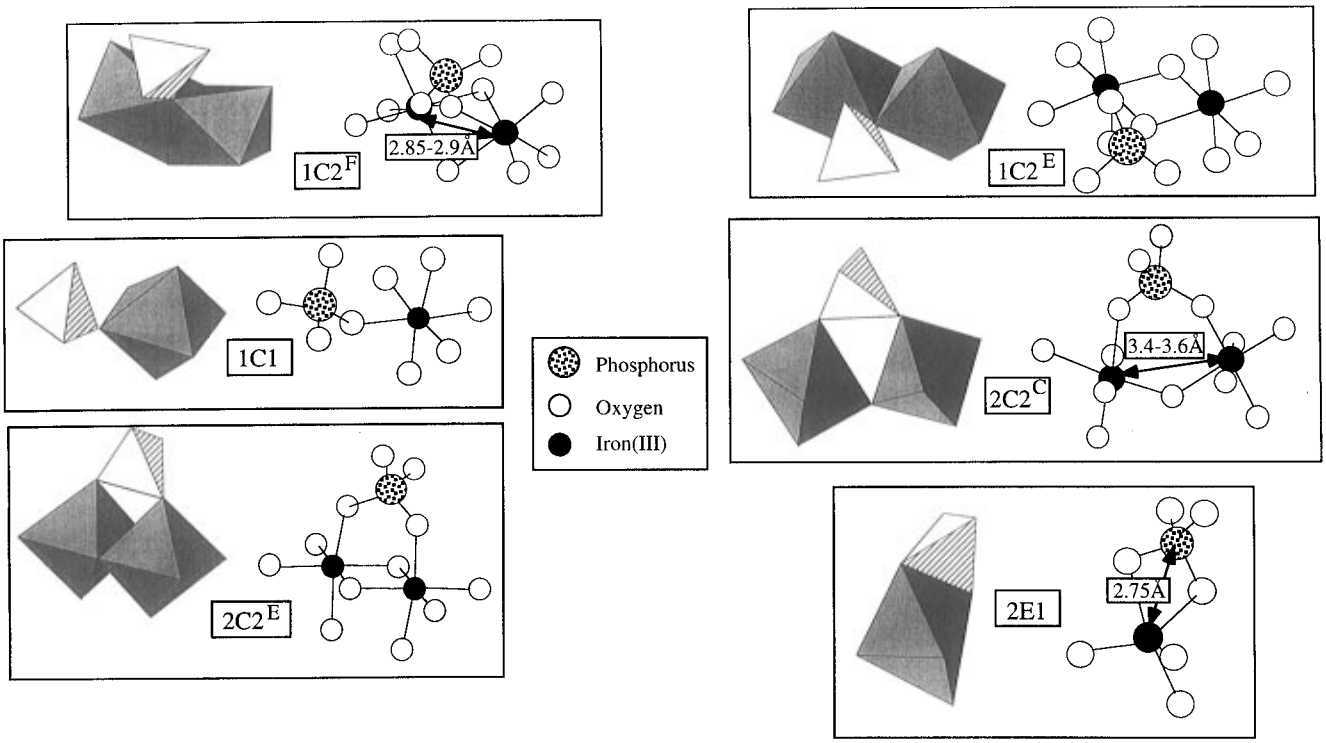

Figure 5. Six different types of linkage between the PO_4 tetrahedron and the Fe(III) octahedron extracted from natural iron/phosphate.

Discussion

Two major problems are encountered in the interpretation of our P K-edge EXAFS data.

(i) The P−Fe distance of 3.05 Å (P/Fe = 0.2, *n* = 1.5, *n* = 2) has not been reported previously in the literature.[6] A set of known Fe−PO_4 structures needs to be examined in terms of bond types and angles to select those which are the most likely to account for this short experimental Fe−P distance.

(ii) The peaks present in the 1.8−2.7 Å range of RDFs (Figure 3) could result for background noise or multiple scattering effects. If these peaks are due to multiple scattering phenomena, it could also affect the peaks corresponding to P−Fe contributions. Thus the contribution of multiple scattering to the overall EXAFS signal must be assessed by *ab initio* calculations of the spectra.

The following discussion will be focused on these two aspects.

Determination of the Topologic Relation between PO_4 Tetrahedron and Fe(III) Octahedron. A large number of iron phosphate minerals has been investigated (barbosalite, lipscombite, $Fe_2(PO_4)Cl$, rockbridgeite, vivianite, whitmoreite, $Fe_3(H_2O)(PO_4)_2$, strengite, $Fe^{2+}Fe^{3+}{}_2(PO_3OH)_4(H_2O)_4$). They can be classified into six modes according to the type of linkage between PO_4 and Fe. Figure 5 illustrates these different cases and their corresponding terminology. The linkages are named on the basis of the number of corners of the tetrahedron involved in the association with Fe(III) and the number of irons in the second coordination sphere. The notation NXM^Y corresponds to the following: *N* is the number of corners of the tetrahedron involved in the linkage, *X* is the type of linkage between polyhedra (i.e., C for corner, E for edge), *M* stands for the number of iron atoms in the second coordination sphere of phosphorus (for one linkage), and *Y* is the type of linkage between iron octahedra (C for corner, E for edge, and F for face), when more than one Fe(III) octahedron is in the second coordination sphere. One PO_4 can link several iron octahedra with different types of linkage. The six linkage families are the $1C2^F$ (barbosalite, lipscombite, $Fe_2(PO_4)Cl$, rockbridgeite), $1C2^E$ (vivianite, whitmoreite, $Fe_3(H_2O)(PO_4)_2$), 1C1 (strengite, $Fe^{2+}Fe^{3+}{}_2(PO_3OH)_4(H_2O)_4$, vivianite, whitmoreite, $Fe_2(PO_4)Cl$), $2C2^C$ (barbosalite, $Fe_3(H_2O)(PO_4)_2$, whitmoreite, lipscombite, rockbridgeite), $2C2^E$ (vivianite, $Fe_3(H_2O)(PO_4)_2$), and 2E1 ($Fe_3(H_2O)(PO_4)_2$). Not all of these types

were present in our systems. The $1C2^F$ is only present in $Fe^{2+}-Fe^{3+}$ minerals, and the data obtained at the Fe K-edge are inconsistent with face-sharing Fe atoms.[6] Thus this linkage mode is excluded from the various linkages possible in the present work. The crystallographic data[12,17−20] show that the $2C2^C$ mode corresponds to a Fe−Fe distance of 3.4−3.6 Å, which was not detected experimentally.[6] Finally the 2E1 type is present only in $Fe_3(H_2O)(PO_4)_2$ when fivefold-coordinated Fe^{2+} is linked to P at 2.75 Å.[17] No such distance was detected in our samples. Therefore in our case we expect three linkage types: viz. $1C2^E$, 1C1, and $2C2^E$.

None of the reference minerals exhibit a P−Fe distance of 3.05 Å. Taking into account Fe−O distances detected experimentally and P−O−Fe angles observed in natural compounds, the shortest possible distance for the $2C2^E$ type is approximately 3.20 Å. Thus this type of linkage can reasonably be excluded. For the other two types of linkage ($1C2^E$, 1C1), it is geometrically possible to obtain such a short distance for small Fe−O−P angles. Nevertheless, we cannot discriminate between these two structures.

Multiple Scattering Approach. The presence of RDF peaks in the 1.8−2.7 Å range (Figure 3) has to be analyzed. If these peaks correspond to background noise, the attribution of peaks present in the 2.7−3.8 Å range (as structural information) becomes questionable. RDF peaks present in the 1.8−2.7 Å range could also correspond to multiple scattering effects. For example a multiple scattering path involving two oxygen atoms of the phosphate tetrahedron, $P-O_1-O_2$, leads to a distance between 2.4 and 2.8 Å. Moreover if a multiple scattering phenomenom exists in this RDF region, it can also affect the entire RDF. Thus a multiple scattering approach was developed using the FEFF601 code.[21] This *ab initio* code allows the recalculation of the $\chi(k)$ general shape by determining separately the contribution of each multiple scattering path and keeping only those which exceed a given threshold. To use this code the exact atomic coordinates of a given cluster are required.

The problem here however is that the EXAFS data at the P K-edge do not provide a precise determination of the P−O distances (phosphate geometry). This is because the spectra are recorded over a too short energy range. The chosen PO_4 geometry corresponds thus to an average structure based on the analysis of a large number of natural PO_4 compounds,[22] and the real structure of the phosphate is only approximated. The structure and atomic coordinates of the phosphate tetrahedron are given in Figure 6. In order to validate the structural information obtained (Table 2), the EXAFS spectra were calculated in a multiple scattering approach, for the six clusters shown in Figure 7. Cluster A corresponds to the association of one phosphate and one iron through a 1C1 type with a P−Fe distance of 3.3 Å. In cluster B one phosphate bridges two irons (through a 1C1 type of linkage) at a P−Fe distance of 3.31 Å. For clusters C, D, and E, three iron octahedra are bridged by one tetrahedron (still through a 1C1 type). Differences only appear in the P−Fe distances. Cluster F exhibits two different kinds of linkages between the PO_4 tetrahedron and the Fe octahedra: 1C1 and $1C2^E$.

(17) Moore, P. B.; Araki, T. *Am. Mineral.* **1975**, *60*, 454−459.
(18) Lindberg, M. L.; Christ, C. L. *Acta Crystallogr.* **1959**, *12*, 695−697.
(19) Moore, P. B.; Anthony, R.; Kampf, A.; Irving, J. *Am. Mineral.* **1974**, *59*, 900−905.
(20) Vencato, I.; Mattievich, E.; Mascarenhas, Y. P. *Am. Mineral.* **1989**, *74*, 456−460.
(21) Rehr, J. J.; Albers, R. C.; Zabinsky, S. I. *Phys. Rev. Lett.* **1992**, *69* (23), 3397.
(22) Corbridge, D. E. C. *Bull. Soc. Fr. Mineral. Cristallogr.* **1971**, *94*, 271−299.

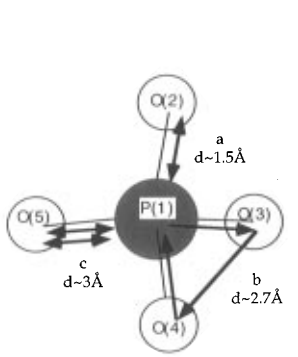

Atomic coordinates

	X	Y	Z
P(1)	0,000	0,000	0,000
O(2)	1,036	-0,109	-1,066
O(3)	-1,063	0,978	-0,473
O(4)	0,655	0,540	1,261
O(5)	-0,607	-1,386	0,336

Exemple of different scattering paths
A : single scattering path
B : triple scattering path
C : quadruple scattering path

Figure 6. Structure of the phosphate chosen for different clusters. Atomic coordinate are given in angstroms. Three scattering paths are presented. a) single scattering path; (b) triple scattering path (distance ~2.7 Å); (c) quadruple scattering path (distance ~ 3 Å).

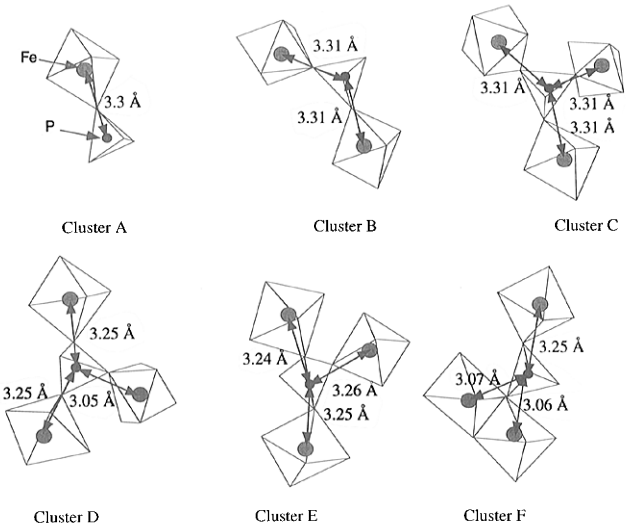

Figure 7. Clusters used for the multiple scattering calculation.

In the companion paper[6] we showed that the majority of iron is involved in the formation of dimers where iron octahedra share one edge and phosphate ions linked one, two, or three of these iron dimers. The six clusters developed for the multiple scattering approach only show linkage between phosphate tetahedra and iron octahedra and not iron dimers. This choice does not mean that phosphate is only in contact with iron monomers. At the P K-edge it is not possible to obtain information at large distances from the central atom, and therefore the presence of the second iron of an iron dimer linked to one phosphate cannot be assessed.

The FEFF601 code was then applied to several models in order to compare calculated with experimental curves for three samples (P/Fe = 0.2, $n = 1$ and 2 and P/Fe = 0.5, $n = 1.5$). For P/Fe = 0.2, the hydrolysis ratios $n = 1$ and $n = 2$ were chosen in order to differentiate the presence of two or three irons around Fe. Moreover the sample P/Fe = 0.2, $n = 2$ was chosen to study the short P−Fe distance. For the other P/Fe series, since there are no significant differences between the spectra, only the sample at $n = 1.5$ was chosen.

P/Fe = 0.2, n = 1. According to EXAFS data (Table 2) it seems that, for this sample, one phosphate is surrounded on average by 1.7 ± 0.2 irons. In a first approximation, we consider that cluster B (one PO_4 linked to two Fe) describes the local structure of this sample.

Importance of Multiple Scattering Paths. Three EXAFS curves were calculated for cluster B with the n_{legs} parameter (number of scattering paths) equal to 2 (single scattering), 3, and 4 (multiple scattering). The adjustment

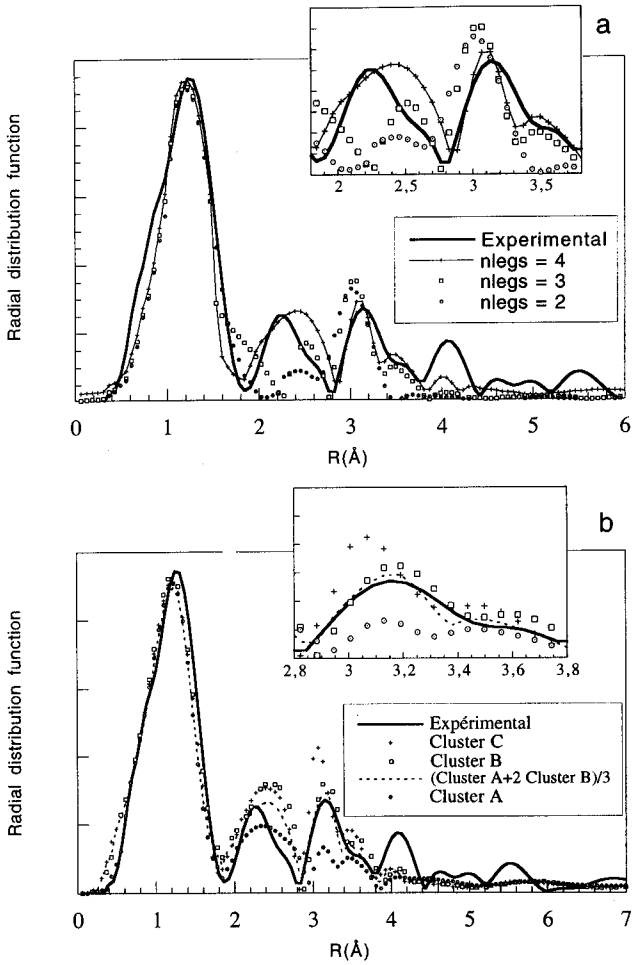

Figure 8. Radial distribution function for P/Fe = 0.2, $n = 1$ and calculated curves including multiple scattering: (a) influence of the multiple scattering path; (b) influence of the number of iron atoms in the second coordination sphere of phosphorus.

of the calculated to the experimental curve implies the introduction of the Debye−Waler factor (σ) in the FEFF601 code. σ chosen for the P−O pair corresponds to the value determined from model compounds (vivianite, rockbridgeite) and was equal to 0.1 Å. For the P−Fe pair, σ was equal to 0.07 Å. For a multiple scattering path involving oxygen atoms or Fe atoms, the σ values were equal to 0.1 Å (the same as for the P−O pair) and 0.07 Å (the same as for the P−Fe pair), respectively. One can note that, for $n_{legs} = 2$ and 3 (Figure 8a), peaks in the 2.7−3.4 Å range of the RDF are not correctly reproduced. With $n_{legs} = 4$ it is possible to reproduce not only the amplitude and shape of these peaks but also the position of the third peak at ≈3.1 Å (distance uncorrected for phase shift). This latter RDF region is better fitted than the 1.8−2.7 Å region. Distances detected in this shorter R range correspond to multiple scattering involving the atoms of the phosphate tetrahedron (Figure 6). The geometry of the phosphate and bond angles strongly influence the shape of the RDF. Since the structure of the PO_4 tetrahedron is not well-known, a perfect fit cannot be expected because of the high number of atomic positions and bonds that need to be considered. Nevertheless it seems that multiple scattering plays an important role in the 1.8−2.7 Å range and that it does not correspond to background noise. For the other calculations the n_{legs} parameter was kept equal to 4. Other authors[23] have also found that this n_{leg} value can reasonably account for multiple scattering effects.

(23) Den Auwer, C. Thesis, Université Paris-Sud 1995, p 237.

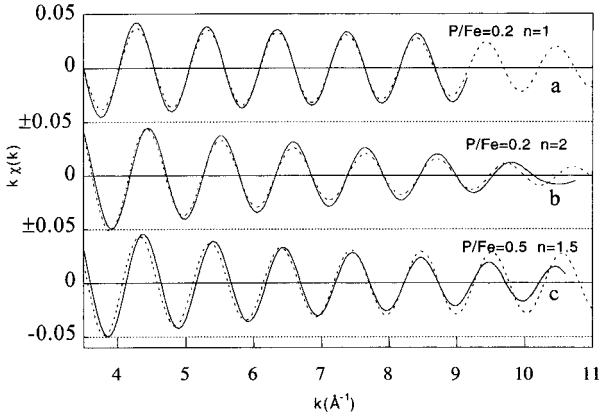

Figure 9. Comparison of partial EXAFS spectra corresponding to the 2.7−3.3 Å range: (a) for the P/Fe = 0.2, $n = 1$ sample; (b) for the P/Fe = 0.2, $n = 2$ sample; (c) for the P/Fe = 0.5, $n = 1.5$ sample. Solid line: experimental spectrum. Doted line: calculated spectrum using the FEFF601 code.

Influence of the Number of Irons in the Second and Third Coordination Spheres of Phosphorus. Because the amplitude of the peak at 3.1 Å is really low (Figure 2), we need to know the accuracy of the number of iron neighbors determined by EXAFS analysis. The experimental EXAFS data for the solution at P/Fe = 0.2, $n = 1$ give 1.7 ± 0.2 Fe_1. Multiple scattering calculations (Figure 8b) were performed with clusters A, B, and C (Figure 7). Large differences between the intensity of the peak at 3.1 Å are found for the three models. Cluster B provides the best agreement with the experimental RDF. Cluster B, however, corresponds to one phosphate tetrahedron surrounded by two iron octahedra. In order to obtain a calculated spectrum with 1.7 irons around the phosphorus, a combination of cluster A (1 iron around phosphorus) and cluster B (2 irons around phosphorus) was considered. The RDF of $(k[(\chi_{\text{cluster A}}(k) + 2\chi_{\text{cluster B}}(k))/3])$ and the partial EXAFS curve corresponding to the 2.7−3.3 Å range of the RDF are in better agreement with the experimental RDF (Figure 8b) and the partial EXAFS spectrum (Figure 9a). However the difference between the RDF calculated for cluster B and the linear combination is not really significant. From these calculations we can reasonably conclude that the major structure in solution is close to cluster B and that some clusters in which one phosphate links one iron are perhaps also present in solution.

Thus, for P/Fe = 0.2, $n = 1$, the structural model assumed from Fe and P K-edge EXAFS experiments is strongly supported by the *ab initio* FEFF601 code.

P/Fe = 0.2, n = 2. For this sample, two P−Fe distances at 3.05 and 3.24 Å were detected by EXAFS analysis (Table 2). First we recalculated the theoretical curve for a species where all P−Fe distances correspond to 1C1 type linkage, i.e. such as in cluster D (Figure 7), but the RDF of this calculated EXAFS spectrum does not agree with the experimental one (Figure 10a). The short P−Fe distance probably does not correspond to a 1C1 PO_4−Fe linkage type. In order to improve the fit, several structures were combined in the calculation: cluster F shows $1C2^E$ and 1C1 linkage type, and the average (cluster F + cluster E)/2 structure corresponds to EXAFS data. The RDF of $(k[(\chi_{\text{cluster E}} + \chi_{\text{cluster F}})/2])$ (Figure 10a) and the partial EXAFS curve (Figure 9b) corresponding to the third peak (see arrow in Figure 10a) agree better with the experimental curves. This calculation shows that it is possible to differentiate between two kinds of PO_4−Fe linkages using the FEFF601 code. Thus the attribution of the short P−Fe distance to a $1C2^E$ instead of a 1C1 type of P−Fe linkage appears to be reasonable.

P/Fe = 0.5, n = 1.5. For this sample it seems that two irons are bridged by one phosphate. For the calculation

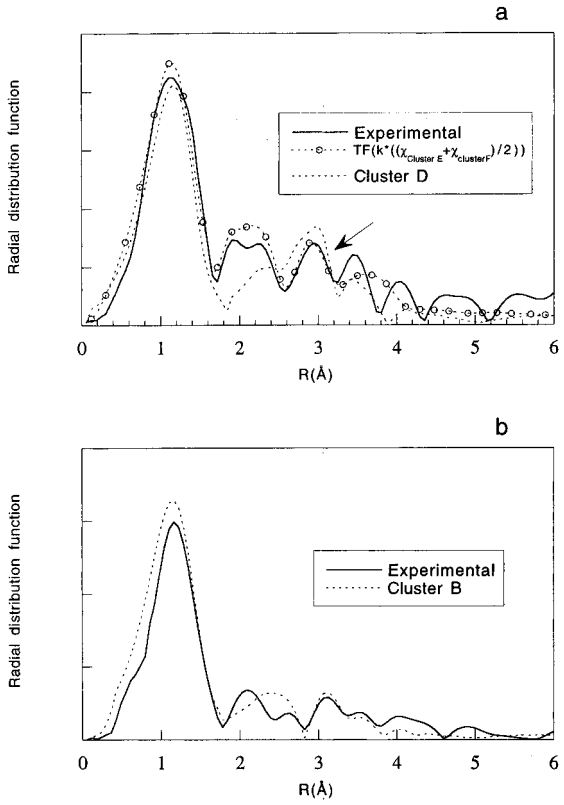

Figure 10. Comparison of the radial distribution function for (a) P/Fe = 0.2, $n = 2$ and (b) P/Fe =0.5, $n = 1.5$ between experimental and calculated curves including multiple scattering. Solid line: experimental spectrum. Doted line: calculated spectrum using the FEFF601 code. Arrow indicates the agreement between experimental and calculated curves.

cluster B was used. Figures 10B and 9C show the comparison of calculated and experimental RDFs and the partial EXAFS curve, respectively. For this sample the agreement is also quite good and validates the structural assumption made.

The multiple scattering approach used at the P K-edge allows us to quantify the importance of this phenomenon, which affects the 1.8−2.7 Å region of RDFs of $PO_4/FeCl_3$ clusters. Moreover, this calculation is sensitive to the type of linkage between one phosphate and several iron octahedra. For the Fe−P system, it is possible to differentiate a 1C1 from a $1C2^E$ P−Fe linkage.

Structure of Clusters during the Growth of Particles. For both P/Fe series, by combining EXAFS data at the Fe and P K-edge, it is possible to propose a Fe−P speciation model all along the hydrolysis process.

For P/Fe = 0.2, at $n = 0$, a P−Fe contribution can be detected (Table 2), but Fe−Fe interactions do not exist.[6] This indicates that only monomeric iron is present in solution and that some Fe octahedra are linked to PO_4. At $n = 1$ each phosphate is surrounded on average by 1.7 ± 0.2 iron atoms, and approximately 30% of the iron octahedra are involved in the formation of the edge-sharing Fe dimer.[6] Thus the solution probably contains a mixture of small oligomers: iron monomers and dimers, one phosphate bridging one or two irons which are either monomeric or dimeric. All phosphate ions are complexed with Fe. As n increases, the majority of the iron atoms are involved in the formation of edge-sharing dimers and the phosphate bridges two to three Fe dimers for $n = 1.5$ and 2, respectively.[6] At the same time the P−Fe distance decreases and at $n = 2$ two types of linkage between PO_4 tetrahedra and iron octahedra are observed ($1C2^E$ and 1C1 and E and F clusters). This may result in a more dense local structure.

At P/Fe = 0.5, we find PO_4-Fe associations even at low n ratios. For $n = 1$, P K-edge EXAFS data suggest that one phosphate is surrounded by approximately one iron. This is close to the Fe K-edge EXAFS results, showing 0.8 phosphorus around Fe. This means that one phosphate is surrounded by more than one Fe (≥1.5). This difference between both EXAFS data could originate from an overestimation of the phosphorus number around Fe by Fe K-edge EXAFS spectroscopy. This overestimation results from the difference in atomic number between Fe and P, making it difficult to quantify the presence of phosphorus by Fe K-edge spectroscopy. For the other hydrolysis ratios the previous study shows that the majority of the iron atoms are involved in the formation of Fe dimers by edge sharing.[6] When $n \geq 1.5$, the growth of the particles could be achieved by Fe octahedra bridging small basic units consisting of phosphate ions bridging two iron dimers.

Conclusion

For the P/Fe = 0.2 series a 3D model is proposed for the structural evolution of colloids during hydrolysis. Clusters are formed from 1C1 and $1C2^E$ type linkage mode between PO_4 and Fe^{3+}. As hydrolysis increases from $n = 0$ to $n = 2$, the number of Fe atoms in the second coordination sphere of P increases from 1.6 to 3.2, respectively. The coordination number increase corresponds to the growth of clusters.[6]

For the P/Fe = 0.5 series, only the 1C1 mode seems to be present as n increases from 0 to 2. The number of Fe^{3+} ions in the second coordination sphere remains unchanged and equal to 2 when $n \geq 1.5$. The growth of the clusters and the gelation occurring at $n = 2$ suggest an atomic mechanism which involves the bridging of PO_4/Fe clusters through Fe^{3+} bridges.[6]

These new results and the new 3D nucleation and growth model developed here have been obtained by combining EXAFS data at the Fe and P K-edge with the multiple scattering approach (in order to validate P K-edge EXAFS data). To our knowledge this complementary approach has not yet been reported and should be developed for many amorphous systems implying heavy and light elements. The multiple scattering approach appears to be essential in such systems, in order to extract precise detailed local structural information for the lighter elements.

Acknowledgment. This work is a partial fulfillment of a Ph.D. thesis. It was financially supported by Elf-Atochem company. It was also achieved through an EEC exchange research program within the COST action n°D5 "Chemistry at Surfaces and Interfaces". The authors wish to thank the team in charge at the EXAFS SA 32 line of the Super ACO synchrotron for helpful and kind assistance, M. Pompa for technical assistance, and P. Lagarde for fruitful discussions and suggestions. We also thank A. Heurtel for technical support during the development of the measuring cells.

LA961039D